**EUROPEAN JOURNAL OF PURE AND APPLIED MATHEMATICS**
2025, Vol. 18, Issue 2, Article Number 6104
ISSN 1307-5543 – ejpam.com
Published by New York Business Global

# Gender-Specific Modeling for Lassa Virus Transmission with Hearing Loss Disability Risk and Control Strategies

Kamel Guedri[1], Yasir Ramzan[2,3], Muhammad Mudassar Bilal[3], Hatoon Abdullah Niyazi[4,5], Aziz Ullah Awan[3,*], Basim M. Makhdoum[1]

[1] *Mechanical Engineering Department, College of Engineering and Architecture, Umm Al-Qura University, P. O. Box 5555, Makkah 21955, Saudi Arabia*
[2] *Department of Mathematics, Shanghai University, 99 Shangda Road, Shanghai, 200444, China*
[3] *Institute of Mathematics, University of the Punjab, Lahore 54590, Pakistan*
[4] *Department of Clinical Microbiology and Immunology, Faculty of Medicine, King Abdulaziz University, Jeddah 21589, Saudi Arabia*
[5] *King Salman Center for Disability Research, Riyadh 11614, Saudi Arabia*

**Abstract.** This study examines the transmission with hearing loss disability risk of Lassa fever using a gender-spesific model based on nonlinear differential equations. The human population is divided into susceptible females, infected females, susceptible males, infected males, and recovered humans. Empirical data from LASV-endemic regions are employed for rigorous validation and parameter estimation, ensuring alignment with observed cases. The basic reproduction number $R_0$, obtained using the next-generation matrix approach, functions as a necessary limit to quantify outbreak prospects and evaluate control efficacy. Sensitivity analysis identifies dominant transmission drivers such as rodent-human contact rate. Analyzing optimal control techniques using Pontryagin's maximum principle, assess the impact of time-dependent interventions such as rodent population suppression and community-led hygiene education.

**2020 Mathematics Subject Classifications**: 34D23, 34H05
**Key Words and Phrases**: Lassa virus, Disability risk, Reproduction number, Parameter estimation, Sensitivity analysis, Optimal control

## 1. Introduction

Lassa fever is a hemorrhagic illness carried by rats, with its origins traced back to Nigeria [1]. It has existed in Nigeria since the 1950s. It received notice in 1969 when two nurses succumbed to the illness in Lassa town, located in Borno State [2]. This disease is mostly confined to West Africa and constitutes a severe regional health challenge, resulting in substantial annual morbidity and mortality.

The elimination of the Lassa virus in West Africa remains difficult because of the unpredictability of recovery. The virus can stay in human body secretions, such as sperm, even after recovery [3]. Cases of Lassa fever are most prevalent in Nigeria, Liberia, Sierra Leone, and Guinea. Mastomys natalensis is widespread across these regions. The Lassa virus primarily spreads to humans through contact with Mastomys rodent urine or by eating infected food, as shown in Figure 1. Sexual contact is another way that the Lassa virus spreads. The virus can be identified in semen during the healing phase. Infection can also occur through open cuts or wounds exposed to the virus [4, 5].

Reports indicate that in certain areas of Liberia and Sierra Leone, approximately 10%–16% of annual hospitalizations are attributed to Lassa fever, highlighting its serious health implications

*Corresponding author.
DOI: https://doi.org/10.29020/nybg.ejpam.v18i2.6104
*Email addresses:* aziz.math@pu.edu.pk (Aziz Ullah Awan)

 

for these populations [6]. Transmission from one individual to another and spread in the lab can occur due to insufficient prevention and control measures [7]. Lassa fever incidence peaks during the dry season despite the reproduction of multimammate rodents occurring during the wet season [8–11].

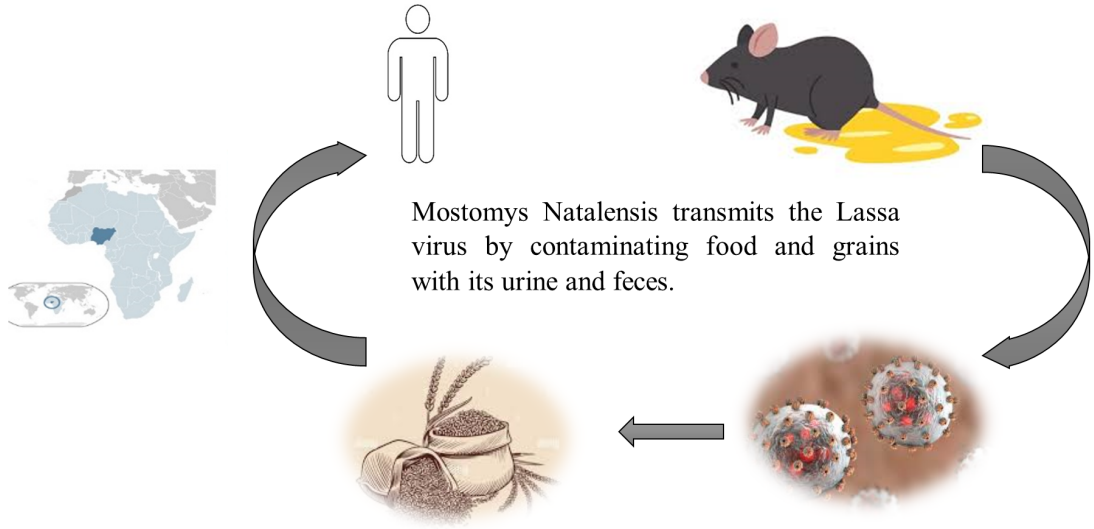


Figure 1: Transmission of Lassa virus

Development duration of Lassa fever ranges from 6 to 21 days. In about 80% of cases, signs are mild and often go unnoticed, including moderate fever, general pain, fatigue, and headaches. However, 20% of infected individuals may experience severe symptoms that can escalate to acute conditions such as respiratory distress, persistent vomiting, severe pain in various body parts, facial disfigurement, and shock [12]. Lassa virus affects around 500,000 people annually and can lead to sudden-onset sensorineural hearing loss in about one-third of survivors. The World Health Organization estimates that 368 million people globally have hearing impairment, primarily in developing countries. Sudden-onset sensorineural hearing loss is characterized by cochlear hair cell or inner ear nerve damage, resulting in a hearing loss of 30 dB or more across at least three frequencies within 72 hours. [13].

Many authors use mathematical modeling to depict various real-life phenomena such as documented in [14–18] . Different models such as [19–22] have been developed for diseases to address specific challenges and enhance our understanding of epidemiological patterns. Onah *et al.* [23], Ibrahim *et al.* [24], and Peter *et al.* [25] earlier proposed optimal Lassa fever control models, but their models did not divide the human population by gender. In contrast, the current study extends previous work by investigating Lassa virus transmission in both human and rodent populations with a novel emphasis on gender-specific categorization in humans. This model addresses viral propagation between genders through sexual interactions, providing a nuanced perspective on how infection pathways may alter depending on sex-based behavioral and biological factors, a feature missing from previous investigations.

This study offers valuable information for governing bodies and healthcare officials by evaluating the impact of different control measures. Additionally, a visual representation of the control strategy is presented. The findings highlight that limiting human-to-human transmission, improving recovery rates, and reducing interactions between humans and infected rodents are crucial steps in bringing the basic reproduction number below one, ultimately helping to control the outbreak. By combining mathematical modeling with real-world epidemiological data, this study enhances the accuracy of disease predictions, providing a strong foundation for

informed decision-making in epidemic management.

## 2. Mathematical Framework

Lassa fever system consists of the human population and rodent population represented by $H(t)$ and $M(t)$ consequently, which are consistent across time. To study Lassa virus transmission, the human population is categorized into five groups such as $F_s(t)$ for susceptible females, $F_i(t)$ for infected females, $M_s(t)$ for susceptible males, $M_i(t)$ for infected males, and $R(t)$ for recovered individuals. The whole human population is expressed as:

$$H(t) = F_s(t) + F_i(t) + M_s(t) + M_i(t) + R(t).$$

Likewise, the species rodent is divided into two groups such as $R_s(t)$ for susceptible rodents and $R_i(t)$ for infected rodents, with the entire rodent population stated as:

$$M(t) = R_s(t) + R_i(t).$$

Individuals are assumed to become part of susceptible classes $F_s(t)$ and $M_s(t)$ along birth at rates $\Pi$ and $\Lambda$ separately. The principal transmission mechanisms are encounters between rats and people and human interactions. It can also be transmitted through sexual interaction among humans [26]. Females and males have rates of rat infestation represented as $\alpha_1$ and $\alpha_2$ while the rate of male-to-female and female to-male transmission is represented like $\beta_1$ and $\beta_2$ individually. Infectious females $F_i(t)$ and males $M_i(t)$ encounter deafness at rates $\delta_1$ and $\delta_2$. Both infectious females $F_i(t)$ and males $M_i(t)$ recovers at rates $\rho_1$ and $\rho_2$.
Additionally, rodents are assumed to fall into the susceptible class $R_s(t)$ along birth at a rate $\Psi$. Susceptible rats can get the Lassa virus by contact with infectious rats $R_i(t)$ at a rate $\phi$. The natural mortality rates for human individuals and rodents are indicated by $\mu$ and $\xi$, respectively. These presumptions developed the differential equations (1) to characterize the problem's biological dynamics. Figure 2 displays the flow diagram for the model (1). The following is the formulation of the differential equation system:

$$\begin{aligned}
\frac{dF_s}{dt} &= \Pi - \frac{\beta_1 F_s M_i}{H} - \frac{\alpha_1 F_s R_i}{M} - \mu F_s,\\
\frac{dF_i}{dt} &= \frac{\beta_1 F_s M_i}{H} + \frac{\alpha_1 F_s R_i}{M} - (\mu + \delta_1 + \rho_1) F_i,\\
\frac{dM_s}{dt} &= \Lambda - \frac{\beta_2 M_s F_i}{H} - \frac{\alpha_2 M_s R_i}{M} - \mu M_s,\\
\frac{dM_i}{dt} &= \frac{\beta_2 M_s F_i}{H} + \frac{\alpha_2 M_s R_i}{M} - (\mu + \delta_2 + \rho_2) M_i,\\
\frac{dR}{dt} &= \rho_1 F_i + \rho_2 M_i - \mu R,\\
\frac{dR_s}{dt} &= \Psi - \phi R_s R_i - \xi R_s,\\
\frac{dR_i}{dt} &= \phi R_s R_i - \xi R_i.
\end{aligned} \tag{1}$$

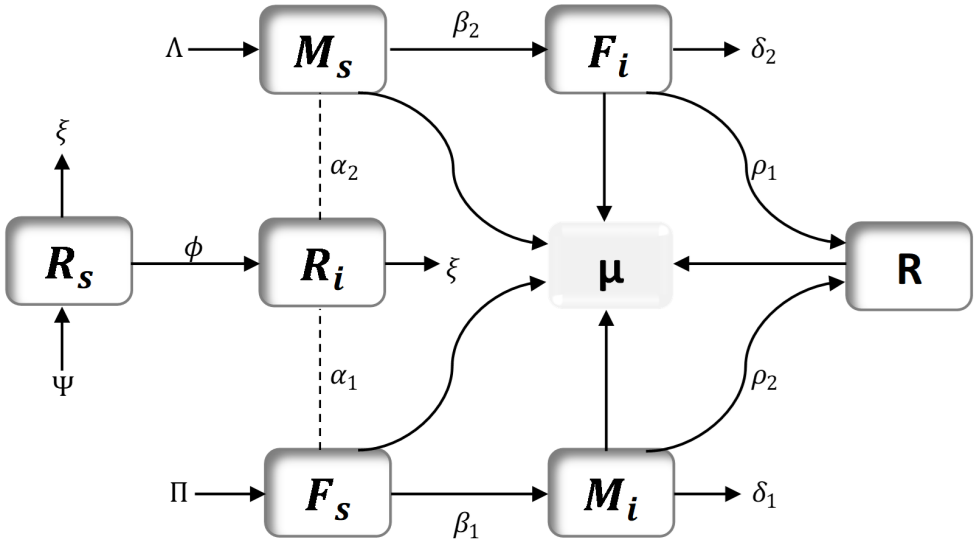


Figure 2: Flow diagram for model (1)

## 2.1. Invariant Region

The interpretation of the invariant region is:

$$\Gamma = \Gamma_h \times \Gamma_r \in \mathbb{R}^5_+ \times \mathbb{R}^2_+,$$

where

$$\Gamma_h = \left\{ (F_s, F_i, M_s, M_i, R) \,|\, H = F_s + F_i + M_s + M_i + R \leq \frac{\Pi + \Lambda}{\mu} \right\}, \tag{2}$$

and

$$\Gamma_r = \left\{ (R_s, R_i) \,|\, M = R_s + R_i \leq \frac{\Psi}{\xi} \right\}. \tag{3}$$

The theorem on local invariant sets [27, 28] supports the statement a certain region Γ has a positive invariance. The region Γ indicates that the mathematical framework of model (1) remaings valid within it.

## 2.2. Basic Reproduction Number ($R_0$)

The likelihood of Lassa fever spreading increases when an individual in the population becomes infected. The basic reproduction number in epidemiology is a critical threshold for disease transmissibility. This metric will be calculated for model (1) to help predict whether an outbreak of Lassa fever will likely occur within the population. The next-generation matrix approach [29] is used to calculate the basic reproduction number $R_0$.

$$R_0 = \max(R_h, R_r), \tag{4}$$

$$R_h = \frac{1}{\Lambda + \Pi} \sqrt{\frac{\Lambda \Pi \beta_1 \beta_2}{(\mu + \delta_1 + \rho_1)(\mu + \delta_2 + \rho_2)}},$$

$$R_r = \frac{\Psi \phi}{\xi^2}.$$

So, $R_h$ & $R_r$ represents the basic reproduction number of rats & humans.

### 2.3. Stability at Disease-Free Equilibrium

This study examines the local stability of the system at disease-free equilibrium (DFE) to measure immediate systemic trends [29, 30]. The disease-free equilibrium of the model (1) can be identified by establishing the derivatives of all infected compartments to zero.

$$(F_s^0, F_i^0, M_s^0, M_i^0, R^0, R_s^0, R_i^0) = \left(\frac{\Pi}{\mu}, 0, \frac{\Lambda}{\mu}, 0, 0, \frac{\Psi}{\xi}, 0\right). \tag{5}$$

At the DFE, the Jacobian matrix $J^0$ is

$$J^0 = \begin{bmatrix} -\mu & 0 & 0 & -\frac{\Pi\beta_1}{\Lambda+\Pi} & 0 & 0 & -\frac{\Pi\xi\alpha_1}{\Psi\mu} \\ 0 & -(\mu+\delta_1+\rho_1) & 0 & \frac{\Pi\beta_1}{\Lambda+\Pi} & 0 & 0 & \frac{\Pi\xi\alpha_1}{\Psi\mu} \\ 0 & -\frac{\Lambda\beta_2}{\Lambda+\Pi} & -\mu & 0 & 0 & 0 & -\frac{\Lambda\xi\alpha_2}{\Psi\mu} \\ 0 & \frac{\Lambda\beta_2}{\Lambda+\Pi} & 0 & -(\mu+\delta_2+\rho_2) & 0 & 0 & \frac{\Lambda\xi\alpha_2}{\Psi\mu} \\ 0 & \rho_1 & 0 & \rho_2 & -\mu & 0 & 0 \\ 0 & 0 & 0 & 0 & 0 & -\xi & -\frac{\phi\Psi}{\xi} \\ 0 & 0 & 0 & 0 & 0 & 0 & \frac{\phi\Psi}{\xi} - \xi \end{bmatrix}.$$

The Jacobian matrix $J^0$ has the following eigenvalues:

$$\lambda_1 = -\mu,$$
$$\lambda_2 = -\xi,$$
$$\lambda_3 = \phi\frac{\Psi}{\xi} - \xi = \xi(R_r - 1),$$
$$\lambda_4 = \frac{-(2\mu+\delta_1+\delta_2+\rho_1+\rho_2) + \sqrt{(2\mu+\delta_1+\delta_2+\rho_1+\rho_2)^2 - 4\left((\mu+\delta_1+\rho_1)(\mu+\delta_2+\rho_2) - \frac{\Lambda\Pi\beta_2}{(\lambda+\Pi)^2}\right)}}{2},$$
$$\lambda_5 = \frac{-(2\mu+\delta_1+\delta_2+\rho_1+\rho_2) - \sqrt{(2\mu+\delta_1+\delta_2+\rho_1+\rho_2)^2 - 4\left((\mu+\delta_1+\rho_1)(\mu+\delta_2+\rho_2) - \frac{\Lambda\Pi\beta_2}{(\lambda+\Pi)^2}\right)}}{2}.$$

Clearly $\lambda_1$, $\lambda_2$ and $\lambda_5$ possess negativity. The expression $\lambda_3$ is also negative when $R_r < 1$. The negativity of $\lambda_4$ can be checked by taking reproduction number

$$R_h = \frac{1}{\Lambda+\Pi}\sqrt{\frac{\Lambda\Pi\beta_1\beta_2}{(\mu+\delta_1+\rho_1)(\mu+\delta_2+\rho_2)}} < 1$$

using

$$\frac{\Lambda\Pi\beta_1\beta_2}{(\Lambda+\Pi)^2} < (\mu+\delta_1+\rho_1)(\mu+\delta_2+\rho_2)$$

$$\lambda_4 < \frac{-(2\mu+\delta_1+\delta_2+\rho_1+\rho_2) + \sqrt{(2\mu+\delta_1+\delta_2+\rho_1+\rho_2)^2 - 4(\mu+\delta_1+\rho_1)(\mu+\delta_2+\rho_2)}}{2}$$

$$\lambda_4 < 0$$

Also, it's clear that $\lambda_4$ has negativity. Negative eigenvalues show the disease's gradual eradication, leading to stability at DFE. Consequently, the following theorem can be utilized to understand.

**Theorem 1.** *When $R_0 < 1$, the model (1) shows local asymptotic stability (LAS) at DFE [31].*

A locally stable DFE is achieved by the population when the basic reproduction number $R_0$ is below 1, indicating a strong possibility of eliminating Lassa fever from the community. This result is of great importance from an epidemiological perspective. However, if $R_0$ exceeds one, the infection persists, establishing an endemic presence in the population. Analyzing the global stability at the disease-free equilibrium is essential to ensuring the disease's elimination irrespective of the initial infection levels.

**Theorem 2.** *The model (1) shows global asymptotic stability (GAS) at DFE for $R_0 < 1$ [31].*

To analyze GAS at DFE, it is enough to verify that conditions $H_1$ and $H_2$ hold when $R_0 < 1$, as detailed in [32]. The model (1) variables are categorized as $M_1 = (F_s, M_s, R_s)$ and $M_2 = (F_i, M_i, R_i)$. Furthermore, the DFE can be represented as $M_1^* = (\frac{\Pi}{\mu}, \frac{\Lambda}{\mu}, \frac{\Psi}{\xi})$. By solving the system of linear equations

**Condition ($H_1$):** The non-infected subsystem $\frac{dM_1}{dt} = F(M_1, 0)$ is (GAS) at the DFE. The non-infected compartments $M_1 = (F_s, M_s, R_s)$ satisfy:

$$\begin{aligned}
\frac{dF_s}{dt} &= \Pi - \mu F_s \implies F_s(t) \to \frac{\Pi}{\mu}, \\
\frac{dM_s}{dt} &= \Lambda - \mu M_s \implies M_s(t) \to \frac{\Lambda}{\mu}, \\
\frac{dR_s}{dt} &= \Psi - \xi R_s \implies R_s(t) \to \frac{\Psi}{\xi},
\end{aligned}$$

All solutions converge to $M_1^* = \left(\frac{\Pi}{\mu}, \frac{\Lambda}{\mu}, \frac{\Psi}{\xi}\right)$ satisfying $H_1$.

**Condition ($H_2$):** The infected subsystem $\frac{dM_2}{dt} = G(M_1, M_2) = AM_2 - \hat{G}(M_1, M_2)$ where $A = D_{M_2} G(M_1^*, 0)$ is Metzler and $\hat{G} \geq 0$. The Jacobian matrix block for $M_2 = (F_i, M_i, R_i)$ at DFE is:

$$A = \begin{bmatrix} -(\mu + \delta_1 + \rho_1) & \frac{\beta_1 \Pi}{\Pi + \Lambda} & \frac{\alpha_1 \Pi \xi}{\mu \Psi} \\ \frac{\beta_2 \Lambda}{\Pi + \Lambda} & -(\mu + \delta_2 + \rho_2) & \frac{\alpha_2 \Lambda \xi}{\mu \Psi} \\ 0 & 0 & \frac{\phi \Psi}{\xi} - \xi \end{bmatrix}.$$

**Metzler Property:** Off-diagonal entries $\frac{\beta_1 \Pi}{\Pi + \Lambda}, \frac{\beta_2 \Lambda}{\Pi + \Lambda} \geq 0$. Diagonal entries are negative if $R_0 < 1$. Thus, $A$ is Metzler. Define $\hat{G}(M_1, M_2) = AM_2 - G(M_1, M_2)$:

$$\hat{G} = \begin{bmatrix} \left(\frac{\Pi}{\Pi + \Lambda} - \frac{F_s}{H}\right) \beta_1 M_i + \left(\frac{\Pi \xi}{\mu \Psi} - \frac{F_s}{M}\right) \alpha_1 R_i \\ \left(\frac{\Lambda}{\Pi + \Lambda} - \frac{M_s}{H}\right) \beta_2 F_i + \left(\frac{\Lambda \xi}{\mu \Psi} - \frac{M_s}{M}\right) \beta_2 R_i \\ \left(\frac{\Psi}{\xi} - R_s\right) \phi R_i \end{bmatrix} \geq 0.$$

Both conditions $H_1$ and $H_2$ hold when $R_0 < 1$. Hence, the system is globally asymptotically stable at DFE. This completes the proof.

## 3. Parametric Estimation

Finding the best parameter within a model to closely match empirical data is the main goal of data fitting and parameter estimation. This procedure involves modifying these parameters to

lessen the differences between expected outcomes and actual observations. Various statistical tools, optimization strategies, and curve-fitting techniques effectively match the model with real-world data. For parameter estimate, data from the Nigeria Centre for Disease Control and Prevention (NCDC) database is used [33], which records Lassa fever cases over the last eight years from 2018 to 2024.

It is important to remember that the number of verified infections keeps increasing as the year progresses, underscoring the urgent need for efficient steps to stop the virus's spread. Nigeria's average life expectancy was 53 years in 2018 [34]. The population of Nigeria was 198387623 in 2018 [35] with 98222504 females [36] and 100165119 males [37]. To determine values for 10 parameters, the model (1) has been calibrated to actual case data, assuming a total rodent population of 500000. After calibration of the model, Figure 3 compares real and estimated confirmed cases sorted by female and male, encompassing seven years of data from 2018 to 2024.

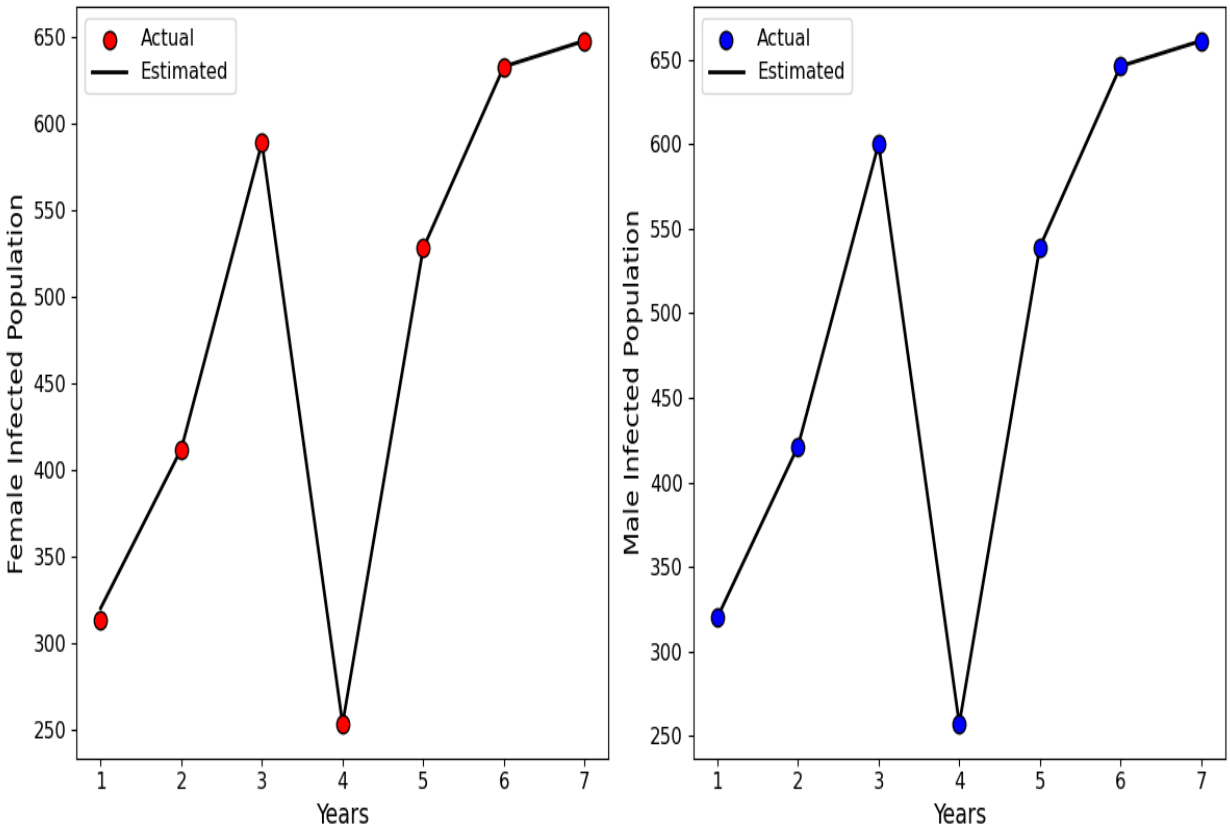


Figure 3: Comparison of estimated and actual cases

In Tables (1) and (2), the estimated parameter values based on the population of different genders and real-world data are provided after calibration with the model. Females' basic reproduction number is between 0.289781 and 4.95163, while for males, it varies from 0.505957 to 7.83412. The basic reproductive number for rodents is 3.4626.

Table 1: Lassa fever model (1) parameters based on the female human population

| Notations | Values | Designation | Source |
|---|---|---|---|
| $\Pi$ | 1853254.8 | Growth rate of female human population | [34, 36] |
| $\Lambda$ | 1889907.9 | Growth rate of male human population | [34, 37] |
| $\Psi$ | 125000 | Growth rate of rodents population | assumed |
| $\mu$ | 0.0188679 | Humans natural mortality rate | [34] |
| $\xi$ | $[0.19, 0.246]$ | Rodents natural mortality rate | fitted |
| $\alpha_1$ | $[2.97 \times 10^{-5}, 3.93 \times 10^{-5}]$ | Rate of infection prevalence among female humans via rodents | fitted |
| $\alpha_2$ | $1 \times 10^{-5}$ | Rate of infection prevalence among male humans via rodents | fitted |
| $\beta_1$ | 0.25 | Rate of infection prevalence from male to female humans | fitted |
| $\beta_2$ | 0.35 | Rate of infection prevalence from female to male humans | fitted |
| $\rho_1$ | $[0.01, 0.245]$ | Rate of recuperation for female humans | fitted |
| $\rho_2$ | $[0.01, 0.246]$ | Rate of recuperation for male humans | fitted |
| $\delta_1$ | $[0.001, 0.246]$ | The rate at which female loss their hearing sense | fitted |
| $\delta_2$ | $[0.001, 0.246]$ | The rate at which male loss their hearing sense | fitted |
| $\varphi$ | 0.000001 | Rate of contamination between rodents | fitted |

Table 2: Lassa fever model (1) parameters based on the male human population

| Notations | Values | Designation | Source |
|---|---|---|---|
| $\Pi$ | 1853254.8 | Growth rate of female human population | [34, 36] |
| $\Lambda$ | 1889907.9 | Growth rate of male human population | [34, 37] |
| $\Psi$ | 125000 | Growth rate of rodents population | assumed |
| $\mu$ | 0.0188679 | Humans natural mortality rate | [34] |
| $\xi$ | 0.19 | Rodents natural mortality rate | fitted |
| $\alpha_1$ | $[2.97 \times 10^{-5}, 6.3 \times 10^{-5}]$ | Rate of infection prevalence among female humans via rodents | fitted |
| $\alpha_2$ | $1 \times 10^{-5}$ | Rate of infection prevalence among male humans via rodents | fitted |
| $\beta_1$ | 0.468 | Rate of infection prevalence from male to female humans | fitted |
| $\beta_2$ | 0.468 | Rate of infection prevalence from female to male humans | fitted |
| $\rho_1$ | $[0.01, 0.2218]$ | Rate of recuperation for female humans | fitted |
| $\rho_2$ | $[0.01, 0.2218]$ | Rate of recuperation for male humans | fitted |
| $\delta_1$ | $[0.001, 0.2218]$ | The rate at which female loss their hearing sense | fitted |
| $\delta_2$ | $[0.001, 0.2218]$ | The rate at which male loss their hearing sense | fitted |
| $\varphi$ | 0.000001 | Rate of contamination between rodents | fitted |

## 4. Sensitivity Analysis

Sensitivity analysis investigates the effects of parameter changes on a model's results. It contributes to the model's robustness by establishing how changes in different parameters affect the findings, identifying key elements, and assessing their overall impact. This analysis is useful for decision-making since it emphasizes the factors significantly impacting the findings, allowing for more accurate and reliable forecasts or choices.

### 4.1. Sensitivity Indices

Sensitivity indices measure how different parameters affect the variables in a given problem. The sensitivity index $\Gamma_x^{R_0}$, which evaluates the impact of each parameter on $R_0$, is computed using the methods described in [38, 39] and is represented by the following equation:

$$\Gamma_x^{R_0} = \frac{\partial R_0}{\partial x} \times \frac{x}{R_0}, \tag{6}$$

Tables (3) and (4) provide an overview of the sensitivity indices. Lassa fever is spread by increasing values of the parameters $\beta_1$ (male to female human infection rate), $\beta_2$ (female to male human infection rate), and $\phi$ (rodent-to-rodent infection rate). Parameters $\rho_1$ (female human recovery rate), $\rho_2$ (male human recovery rate), $\delta_1$ (rate at which female loss their hearing sense),

$\delta_2$ (rate at which male loss their hearing sense) and $\xi$ (rodent mortality rate) inversely influence disease spread. Notably, $\xi$ demonstrates the most significant negative impact, underscoring its role in outbreak mitigation.

Table 3: Parameters of female population's sensitivity indices of $R_0$

| **Notations** | **Description** | **Sensitivity Index** | **Sign** |
|---|---|---|---|
| $\beta_1$ | Rate of infection prevalence from male to female humans | 0.5 | +ve |
| $\beta_2$ | Rate of infection prevalence from female to male humans | 0.5 | +ve |
| $\rho_1$ | Rate of recuperation for female humans | $[-0.240258, -0.167404]$ | -ve |
| $\rho_2$ | Rate of recuperation for male humans | $[-0.240767, -0.167404]$ | -ve |
| $\delta_1$ | The rate at which female loss their hearing sense | $[-0.241239, -0.0167404]$ | -ve |
| $\delta_2$ | The rate at which male loss their hearing sense | $[-0.240767, -0.0167404]$ | -ve |
| $\xi$ | Rodents natural mortality rate | $-2$ | -ve |
| $\phi$ | Rate of contamination between rodents | 1 | +ve |

Table 4: Parameters of male population's sensitivity indices of $R_0$

| **Notations** | **Description** | **Sensitivity Index** | **Sign** |
|---|---|---|---|
| $\beta_1$ | Rate of infection prevalence from male to female humans | 0.5 | +ve |
| $\beta_2$ | Rate of infection prevalence from female to male humans | 0.5 | +ve |
| $\rho_1$ | Rate of recuperation for female humans | $[-0.2398, -0.167404]$ | -ve |
| $\rho_2$ | Rate of recuperation for male humans | $[-0.2398, -0.167404]$ | -ve |
| $\delta_1$ | The rate at which female loss their hearing sense | $[-0.2398, -0.0167404]$ | -ve |
| $\delta_2$ | The rate at which male loss their hearing sense | $[-0.2398, -0.0167404]$ | -ve |
| $\xi$ | Rodents natural mortality rate | $-2$ | -ve |
| $\phi$ | Rate of contamination between rodents | 1 | +ve |

The sensitivity study demonstrates that parameters $\beta_1$ and $\beta_2$, which reflect the infection prevalence among female and male humans via human have a positive sensitivity index, which signifies that if the value increases, it causes a hike in reproduction number. Similarly, the sensitivity analysis demonstrates that parameter $\phi$ representing the infection rate between rodents has a positive sensitivity index, which signifies that the reproduction number would spike if $\phi$ increases. Similarly, the parameter $\xi$ reflects the rodents' natural death rate, and engagement has a negative sensitivity index, which signifies that increasing the value causes a fall in reproduction number.

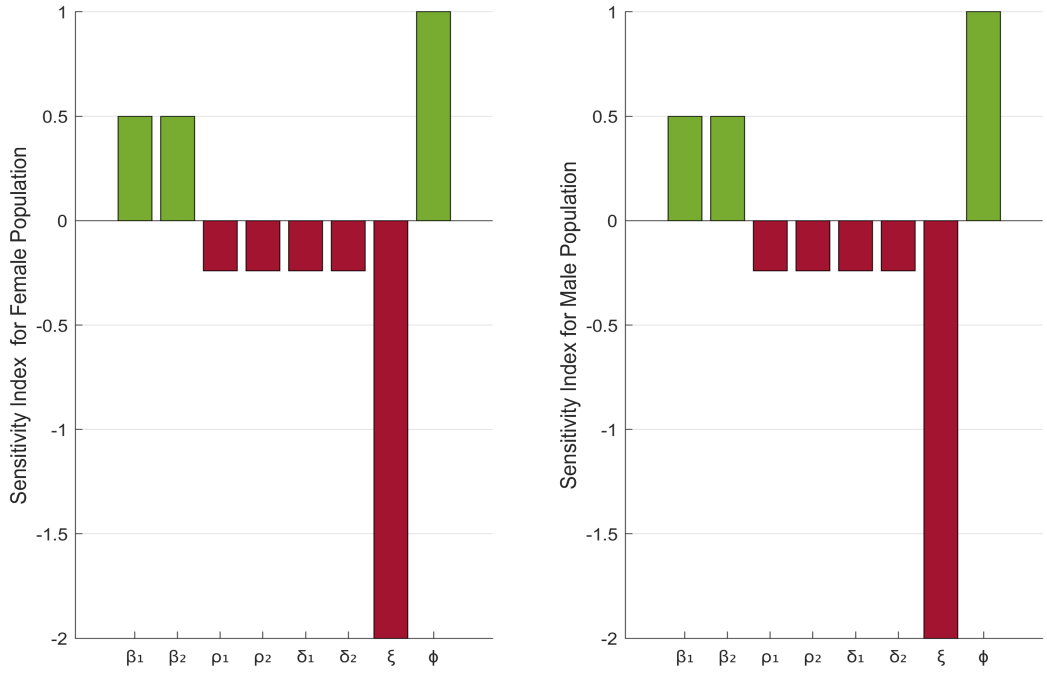


Figure 4: Visual representation of sensitivity indices for the basic reproduction number $R_0$

## 5. Optimal Control

To develop control model (7), four time-varying variables for control $h_1$, $h_2$, $h_3$ and $h_4$ are added to the existing model framework (1). The explanations below provide details about these time-varying control variables:

- The variables $h_1$ and $h_2$ are control measures intended to limit virus transmission from infected rodents to female and male human beings. These precautions include various actions such as educational initiatives to encourage proper hygiene practices, prohibit rat utilization, conduct environmental disinfection, and promote the usage of condoms. It's critical to understand that the efficacy among these measures to restrain infections depends on $h_1$ and $h_2$ to 1. In contrast, providing a zero value to these variables would fail these measures to stop transmission. Hence, effectively executing these precautionary measures is vital to eliminate disease.

- The approach of using technology for mobile healthcare to permit timely identification of possible Lassa-related illness instances from rural or underdeveloped locations is represented by the control variable $h_3$. This can be accomplished by SMS-based programs or mobile applications that enable community members and healthcare professionals to report possible cases promptly and provide timely treatment. Proper utilization of resources and a prompt reaction are made possible by timely reporting, which aids in controlling outbreaks before they get out of control.

- The variable under control of a comprehensive plan to reduce the spread of the virus from infected to vulnerable rats is described in $h_4$. This strategy involves several control methods, including caulking building cracks and gaps, putting wire screens on windows and door frames, catching and eliminating rodents (ideally using live traps), using rodenticides, fumigating infested areas, and possibly bringing in natural predators like dogs, cats, and barn owls.

Based on the descriptions above, an optimal control framework for Lassa fever can be developed by incorporating four time-dependent variables as outlined below:

$$\begin{aligned}
\frac{dF_s}{dt} &= \Pi - \frac{\beta_1 F_s M_i}{H} - (1-h_1)\frac{\alpha_1 F_s I_r}{M} - \mu F_s,\\
\frac{dF_i}{dt} &= \frac{\beta_1 F_s M_i}{H} + (1-h_1)\frac{\alpha_1 F_s I_r}{M} - (\mu+\delta_1+\rho_1)F_i - \theta_1 h_3 F_i,\\
\frac{dM_s}{dt} &= \Lambda - (1-h_2)\frac{\beta_2 M_s F_i}{H} - \frac{\alpha_2 M_s I_r}{M} - \mu M_s,\\
\frac{dM_i}{dt} &= (1-h_2)\frac{\beta_2 M_s F_i}{H} + \frac{\alpha_2 M_s I_r}{M} - (\mu+\delta_2+\rho_2)M_i - \theta_1 h_3 M_i,\\
\frac{dR}{dt} &= \rho_1 I_1 + \rho_2 I_2 - \mu R + \theta_1 h_3 F_i + \theta_1 h_3 M_i,\\
\frac{dR_s}{dt} &= \Psi - \phi(1-\theta_2 h_4)R_s R_i - \xi R_s - \theta_2 h_4 R_s,\\
\frac{dR_i}{dt} &= \phi(1-\theta_2 h_4)R_s R_i - \xi R_i - \theta_2 h_4 R_i.
\end{aligned} \tag{7}$$

The objective is to decrease the Lassa virus's transmission among rats and people in society while preserving affordability by implementing the four control strategies. The framework is defined as follows:

$$G(h_i) = \int_0^{t_f} \left[ Z_1 F_i + Z_2 M_i + Z_3 R_s + Z_4 R_i + \frac{1}{2}\sum_{i=1}^{4} X_i h_i^2(t) \right] dt, \tag{8}$$

Let $t_f$ denote the terminal time for control implementation with $t \in [0, t_f]$. The constant weighting coefficients $Z_1, Z_2, Z_3, Z_4$ and $X_i$ $(i = 1, \ldots, 4)$ quantify the costs associated with the control strategies $h_i$ $(i = 1, \ldots, 4)$. The optimization goal is to find the ideal control quadruplet: $h^* = \{h_1^*, h_2^*, h_3^*, h_4^*\}$,

$$G(h_1^*, h_2^*, h_3^*, h_4^*) = \min\{G(h_1, h_2, h_3, h_4) : h_1, h_2, h_3, h_4 \in \zeta\}, \tag{9}$$

which minimizes the total cost of intervention strategies over the time horizon $[0, t_f]$.

$$\zeta = \{(h_1, h_2, h_3, h_4) : 0 \le h_1(t), h_2(t), h_3(t), h_4(t) \le 1,\ t \in [0, t_f]\}$$

Within the optimum control framework (7), the control reduction problem (9) is transformed into a point-by-point Hamiltonian minimization problem by Pontryagin's maximum principle. The resulting change is studied in detail in [40], and $\mathbb{H}$ is the Hamiltonian equation that results.

$$\mathbb{H} = Z_1 F_i + Z_2 M_i + Z_3 R_s + Z_4 R_i + \frac{1}{2}\sum_{i=1}^{4} X_i h_i^2(t) + \sum_{i=1}^{7} \sigma_i Y_i., \tag{10}$$

Here, adjoint functions connected to state variables of the optimal control system are represented by $\tau_i$ for $i = 1, \ldots, 7$ and the differential equations governing the system's (7) state variables on the right-hand side is represented by $Y_i$ for $i = 1, \ldots, 7$. The following is the extended form

of the Hamiltonian equation:

$$\begin{aligned}\mathbb{H} &= Z_1F_i + Z_2M_i + Z_3R_s + Z_4R_i + \frac{1}{2}X_1h_1^2 + \frac{1}{2}X_2h_2^2 + \frac{1}{2}X_3h_3^2 + \frac{1}{2}X_4h_4^2\\ &+ \tau_1\Big(\Pi - \beta_1\frac{F_sM_i}{H} - (1-h_1)\alpha_1\frac{F_sR_i}{M} - \mu F_s\Big)\\ &+ \tau_2\Big(\beta_1\frac{F_sM_i}{H} + (1-h_1)\alpha_1\frac{F_sR_i}{M} - (\mu+\delta_1+\rho_1)F_i - \theta_1h_3F_i\Big)\\ &+ \tau_3\Big(\Lambda - (1-h_2)\beta_2\frac{M_sF_i}{H} - a_2\frac{M_sR_i}{M} - \mu M_s\Big)\\ &+ \tau_4\Big((1-h_2)\beta_2\frac{M_sF_i}{H} + a_2\frac{M_sR_i}{M} - (\mu+\delta_2+\rho_2)M_i - \theta_1h_3M_i\Big)\\ &+ \tau_5\Big(\rho_1F_i + \rho_2M_i - \mu R + \theta_1h_3F_i + \theta_1h_3M_i\Big)\\ &+ \tau_6\Big(\Psi - \phi(1-\theta_2h_4)R_sR_i - \xi R_s - \theta_2h_4R_s\Big)\\ &+ \tau_7\Big(\phi(1-\theta_2h_4)R_sR_i - \xi R_s - \theta_2h_4R_i\Big)\end{aligned}$$

The subsequent theorem outlines the command $h^*$ that addresses the challenge of minimization (9). It's vital to remember that the method utilized here is based on the techniques covered in [41, 42].

**Theorem 3.** *The following system of equations is satisfied by a collection of adjoint functions $\tau_1(t), \tau_2(t), \ldots, \tau_7(t)$ if there is an optimal control set $h_1^*, h_2^*, h_3^*, h_4^* \in \zeta$ that satisfies (9) concerning the associated state system (7) as outlined in [42]:*

$$\frac{d\tau_1}{dt} = \tau_1\mu + (\tau_1-\tau_2)\frac{\alpha_1R_i}{M} + (\tau_1-\tau_2)\frac{\beta_1M_i}{H} - (\tau_1-\tau_2)h_1\frac{\alpha_1R_i}{M}$$

$$\frac{d\tau_2}{dt} = -Z_1 + \tau_2\mu + \tau_2\delta_1 + (\tau_2-\tau_5)\rho_1 + (\tau_3-\tau_4)\frac{\beta_2M_s}{H} + (\tau_2-\tau_5)\theta_1h_3 - (\tau_3-\tau_4)h_2\frac{\beta_2M_s}{H}$$

$$\frac{d\tau_3}{dt} = \tau_3\mu + (\tau_3-\tau_4)\frac{\alpha_2R_i}{M} + (\tau_3-\tau_4)\frac{\beta_2F_i}{H} - (\tau_3-\tau_4)h_2\frac{\beta_2F_i}{H}$$

$$\frac{d\tau_4}{dt} = -Z_2 + \tau_4\mu + \tau_4\delta_2 + (\tau_4-\tau_5)\rho_2 + (\tau_1-\tau_2)\frac{\beta_1F_s}{H} + (\tau_4-\tau_5)\theta_1h_3$$

$$\frac{d\tau_5}{dt} = \tau_5\mu$$

$$\frac{d\tau_6}{dt} = -Z_3 + \tau_6\xi + (\tau_6-\tau_7)\phi R_i + \tau_6\theta_2h_4 - (\tau_6-\tau_7)\phi I_r\theta_2h_4$$

$$\frac{d\tau_7}{dt} = -Z_4 + \tau_7\xi + (\tau_6-\tau_7)R_s\phi + (\tau_1-\tau_2)\alpha_1F_s + (\tau_3-\tau_4)\alpha_2M_s + \tau_7\theta_2h_4 - (\tau_1-\tau_2)\alpha_1F_sh_1 - (\tau_6-\tau_7)R_s\phi\theta$$

*Under the specified boundary limits:*

$$\tau_i(t_f) = 0 \quad \forall\ i = 1, 2, \ldots, 7,$$

*The derived set is determined as follows:*

$$h^* = (h_1^*, h_2^*, h_3^*, h_4^*)\,.$$

$$
\begin{aligned}
h_1^* &= \min\left\{\max\left\{0, \frac{(\tau_2-\tau_1)}{X_1}\alpha_1\frac{F_sR_i}{M}\right\},1\right\},\\
h_2^* &= \min\left\{\max\left\{0, \frac{(\tau_4-\tau_3)}{X_2}\beta_2\frac{M_sR_i}{H}\right\},1\right\},\\
h_3^* &= \min\left\{\max\left\{0, \frac{(\tau_2-\tau_5)\theta_1F_i+(\tau_4-\tau_5)\theta_1M_i}{X_3}\right\},1\right\},\\
h_4^* &= \min\left\{\max\left\{0, \frac{(\tau_7-\tau_6)\phi\theta_2R_sR_i+(\tau_6R_s+\tau_7R_i)\theta_2}{X_4}\right\},1\right\}.,
\end{aligned}
\tag{11}
$$

*Proof.* Pontryagin's maximal principle can be used to establish the conditions for the existence of the optimal control problem by utilizing the technique described in [41]. To determine the adjoint variables, the partial derivatives of the Hamiltonian function must be evaluated for the state variables.

$$
\begin{aligned}
&\frac{d\tau_1}{dt} = -\frac{\partial H}{\partial F_s}, \quad \frac{d\tau_2}{dt} = -\frac{\partial H}{\partial F_i}, \quad \frac{d\tau_3}{dt} = -\frac{\partial H}{\partial M_S},\\
&\frac{d\tau_4}{dt} = -\frac{\partial H}{\partial M_i}, \quad \frac{d\tau_5}{dt} = -\frac{\partial H}{\partial R}, \quad \frac{d\tau_6}{dt} = -\frac{\partial H}{\partial R_s},\\
&\frac{d\tau_7}{dt} = -\frac{\partial H}{\partial R_i}.
\end{aligned}
$$

Differentiating the Hamiltonian $H$ with respect to the optimal control quadruplet $h^* = (h_1^*, h_2^*, h_3^*, h_4^*)$ within the control set $\zeta$ can determine the behaviour of the controls. Considering the condition $\tau_i(t_f) = 0 \ \forall \ i = 1, 2, \ldots, 7$.

$$
\frac{\partial H}{\partial h_i} = 0, \quad i = 1, 2, \ldots, 4.
$$

By using basic logic to attach restrictions on the values they contain, the controls can now be defined

$$
h_i = \begin{cases} 0, & \text{if } \Delta_i \leq 0, \\ \Delta_i^*, & \text{if } 0 \leq \Delta_i \leq 1, \\ 1, & \text{if } \Delta_i \geq 1. \end{cases}
$$

$$
\begin{aligned}
\Delta_1 &= \frac{(\tau_2-\tau_1)R_i\alpha_1F_s}{X_1},\\
\Delta_2 &= \frac{(\tau_4-\tau_3)\beta_1F_iM_s}{X_2},\\
\Delta_3 &= \frac{(\tau_2-\tau_5)\theta_1F_i+(\tau_4-\tau_5)\theta_1M_i}{X_3},\\
\Delta_4 &= \frac{(P\tau_6+Q\tau_7)\theta_2-(\tau_6-\tau_7)R_sR_i\phi\theta_2}{X_4}.
\end{aligned}
$$

This brings the proof to its conclusion.

The problem has been solved numerically, and the efficacy of the controls put in place has been evaluated. With the information in Tables (1) and (2), it is estimated that the ideal campaign will run for 15 years. Positive weights have been set to $Z_1 = 1$, $Z_2 = 5$, $Z_3 = 10$, $Z_4 = 15$, $X_1 = 3$, $X_2 = 6$, $X_3 = 9$, and $X_4 = 12$. Where, $F_s(0) = 103084231$, $F_i(0) = 9$, $M_s(0) = 105243174$, $M_i(0) = 9$, $R(0) = 50$, $R_s(0) = 500000$, and $R_i(0) = 10000$ are the initial conditions. The objective of implementing all control measures is to minimize the number of victims while increasing the number of recovered individuals, as demonstrated by graphical representations.

## 5.1. Control Effects

The best possible control utilizing the baseline parameter values is shown in Figure 5, providing a comprehensive view of the effectiveness of various intervention strategies. As shown in Figures 5a and 5b, implementing preventive measures at the onset significantly impacts the susceptible human population. Initially, as these measures take effect, susceptible females and males transition into other compartments, leading to a noticeable decline in their numbers.

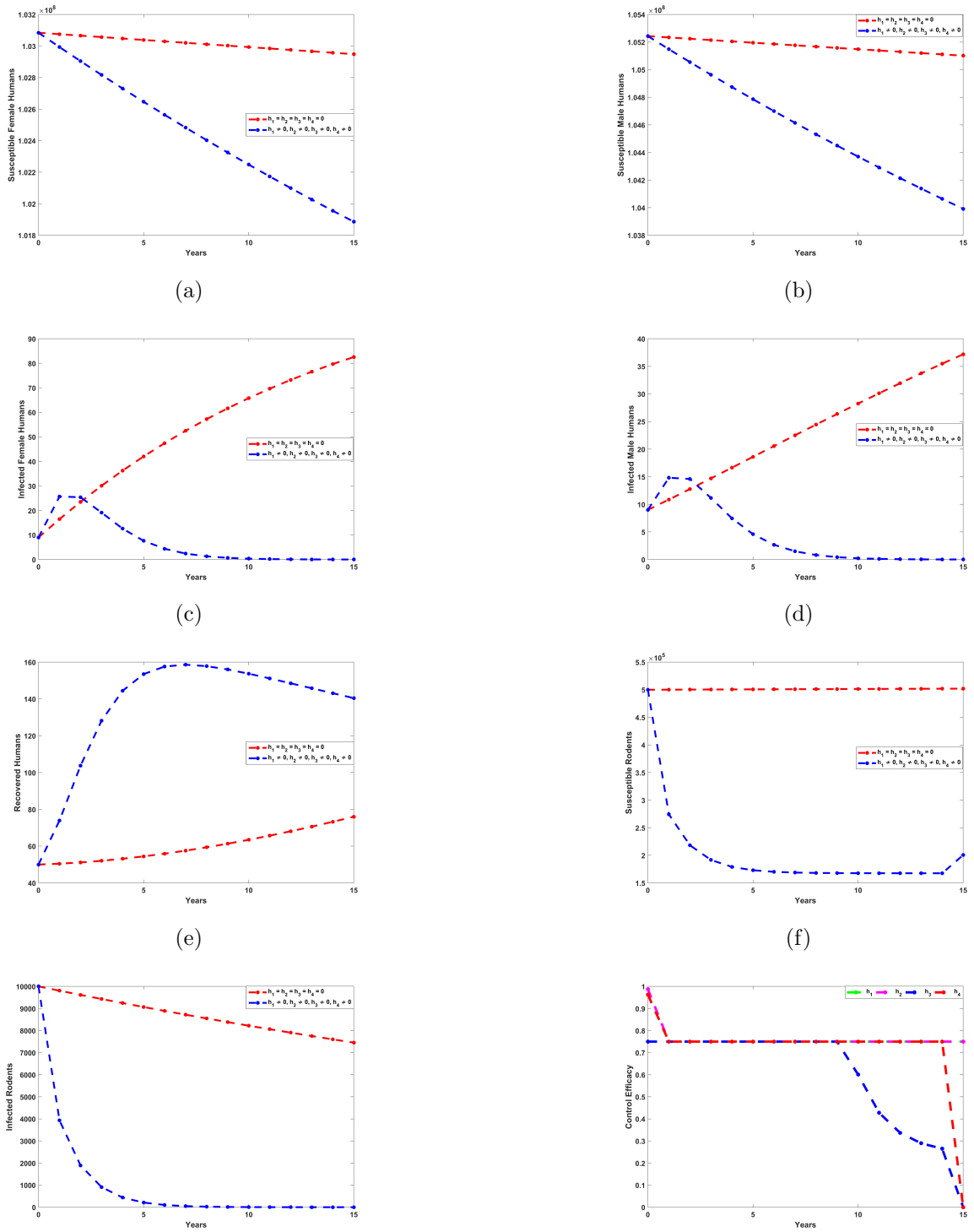


(a) (b) (c) (d) (e) (f) (g) (h)

Figure 5: Visualization of controls $h_1, h_2, h_3, h_4$

The effect of these controls on the infected population is evident in Figures 5c and 5d, which display a notable decline in the overall amount of female and male affected people, respectively. This decline indicates that the control strategies slow down new infections, enhance recovery rates and limit transmission. This leads to a significant rise in the amount of people recovering from the illness, as seen in Figure 5e. The growing population of recovered individuals suggests that applied interventions such as medical treatment, awareness campaigns, and preventive measures are important in mitigating the spread of Lassa fever and enhancing public health outcomes.

Moreover, the effect of these control measures is not limited to the human population alone. Figure 5f demonstrates how applying these interventions reduces the number of susceptible rodents with time. The control measures continue to be used, indicating the effectiveness of rodent-targeted interventions such as habitat control and rodenticides. Similarly, Figure 5g reveals a significant decrease in the number of diseased rodents, further reinforcing the success of these measures in reducing the reservoir population of the Lassa virus.

Finally, numerical findings that demonstrate the overall efficacy of different optimal control measures in controlling the spread of Lassa fever are presented in Figure 5h. The results demonstrate that every action substantially slows the virus's long-term spread. Especially control $h_2$ depicts the best efficacy starting by 100% at the first year and then stabilizes at 75% efficacy for the next 14 years. By assessing these tactics, the study offers insightful information on the best methods for disease control, which eventually helps public health officials create well-informed policies to fight Lassa fever.

## 6. Conclusion

This study comprehensively explores Lassa fever transmission dynamics across human populations by taking a mathematical model on opposite gender and rodent reservoirs, demonstrating its biological validity through evidence of a positively invariant solution and stability at disease-free equilibrium. The model is calibrated with real-world epidemiological data to estimate essential parameters, allowing accurate forecasts of the basic reproduction number ($R_0$).

A sensitivity analysis revealed additional high-impact parameters, such as rodent mortality ($\xi$) and inter-species transmission rates ($\beta_1, \beta_2$), disproportionately influencing outbreak trajectories. Based on these findings, cost-effective intervention techniques are developed, including targeted health campaigns, mobile technologies for early detection, structural pest-proofing, and rodent population control by trapping and rodenticides. Finally, graphical simulations assessed the efficacy of these controls, revealing their ability to reduce illness prevalence significantly and emphasizing the practicality of the proposed treatments in mitigating Lassa fever epidemics.

These findings bridge theoretical modeling and actionable public health practice, equipping policymakers with evidence-based tools to mitigate outbreaks. By synergizing stability analysis, parameter estimation, and sensitivity-driven control design, this work underscores the transformative role of interdisciplinary mathematical approaches in addressing complex health challenges.

Future directions include expanding the model to incorporate climate and mobility factors, conducting real-world trials of interventions, and integrating socioeconomic determinants to refine predictions and improve control strategies.

## Funding

The authors extend their appreciation to the King Salman Center For Disability Research for funding this work through Research Group no KSRG-2024-191.

## Declarations

### Competing Interest

The authors declare no competing interests.

### Declaration of generative AI in scientific writing

All authors declare to no use of AI-assisted technologies in article writing process.

### Data Availability

The data used to support the findings of this study is included within the article.

### Ethical Approval

All the authors declare that our manuscript fulfills all ethical research standards.

## References

[1] D Sambo and CE Madubueze. Mathematical Model of the Transmission Dynamics of Lassa Fever Infection with Controls. *Mathematical Modelling and Applications*, 5(2):65–86, 2020.

[2] V Amorosa, A MacNeil, R McConnell, A Patel, KE Dillon, K Hamilton, BR Erickson, S Campbell, B Knust, D Cannon, D Miller, C Manning, PE Rollin, ST Nichol. Imported Lassa Fever, Pennsylvania, USA. *Emerging Infectious Diseases*, 16(10):1598–1600, 2010.

[3] S Baize, P Marianneau, MC Georges-Courbot, V Deubel. Recent Advances in Vaccines Against Viral Haemorrhagic Fevers. *Current Opinion in Infectious Diseases*, 14(5):513–518, 2001.

[4] VN Raabe, G Kann, BS Ribner, A Morales, JB Varkey, AK Mehta, GM Lyon, S Vanairsdale, K Faber, S Becker, M Eickmann,T Strecker, S Brown, K Patel, PD Leuw, G Schuettfort, C Stephan, H Rabenau, JD Klena, PE Rollin, A McElroy, U Ströher, S Nichol, CS Kraft, T Wolf. Favipiravir and Ribavirin Treatment of Epidemiologically Linked Cases of Lassa Fever. *Clinical Infectious Diseases*, 65(5):855–859, 2017.

[5] A Thielebein, Y Ighodalo, A Taju, T Olokor, R Omiunu, R Esumeh, P Ebhodaghe, A Ekanem, G Igenegbale, R Giwa, A Renevey, J Hinzmann, J Müller, E Pallasch, M Pahlmann, J Guedj, J Nwatuzor, OF Babatunde, DI Adomeh, D Asogun, N Akpede, S Okogbenin, S Günther, L Oestereich, S Duraffour, EO Emovon. Virus Persistence After Recovery from Acute Lassa Fever in Nigeria: A 2-year Interim Analysis of a Prospective Longitudinal Cohort Study. *The Lancet Microbe*, 3(1):e32–e40, 2022.

[6] NS Crowcroft. Management of Lassa Fever in European Countries. *Euro Surveillance*, 7(3):50–52, 2002.

[7] D Cummins, D Bennett, SP Fisher-Hoch, B Farrar, SJ Machin, JB McCormick. Lassa Fever Encephalopathy: Clinical and Laboratory Findings. *The Journal of Tropical Medicine and Hygiene*, 95(3):197–201, 1992.

[8] AH Demby, A Inapogui, K Kargbo, J Koninga, K Kourouma, J Kanu, M Coulibaly, KD Wagoner, TG Ksiazek, CJ Peters, PE Rollin, DG Bausch. Lassa Fever in Guinea: II. Distribution and Prevalence of Lassa Virus Infection in Small Mammals. *Vector Borne and Zoonotic Diseases*, 1(4):283–297, 2001.

[9] KM Johnson, JB McCormick, PA Webb, ES Smith, LH ElliottIJ King. Clinical Virology of Lassa Fever in Hospitalized Patients. *The Journal of Infectious Diseases*, 155(3):456–464, 1987.

[10] L Bolzoni, AP Dobson, M Gatto, GA De Leo. Allometric Scaling and Seasonality in the Epidemics of Wildlife Diseases. *The American Naturalist*, 172(6):818–828, 2008.

[11] CJ Dugaw, A Hastings, EL Preisser, DR Strong. Seasonally Limited Host Supply Generates Microparasite Population Cycles. *Bulletin of Mathematical Biology*, 66(3):583–594, 2004.
[12] IS Abdulraheem. Public Health Importance of Lassa Fever Epidemiology, Clinical Features and Current Management Review of Literature. *African Journal of Clinical And Experimental Microbiology*, 3(1):33–37, 2002.
[13] EJ Mateer, C Huang, NY Shehu, S Paessler. Lassa Fever-Induced Sensorineural Hearing Loss: A Neglected Public Health and Social Burden. *PLoS Neglected Tropical Diseases*, 12(2):e0006187, 2018.
[14] WA Khan, R Zarin, A Zeb, Y Khan, A Khan. Navigating Food Allergy Dynamics via a Novel Fractional Mathematical Model for Antacid-Induced Allergies. *Journal of Mathematical Techniques in Modeling*, 1(1), 2024.
[15] K Abuasbeh, R Shafqat, A Alsinai, M Awadalla. Analysis of the Mathematical Modelling of COVID-19 by Using Mild Solution with Delay Caputo Operator. *Symmetry*, 15(2):286, 2023.
[16] QT Ain, A Din, X Qiang, Z Kou. Dynamics for a Nonlinear Stochastic Cholera Epidemic Model under Lévy Noise. *Fractal and Fractional*, 8(5):293, 2024.
[17] A Sami, A Ali, R Shafqat, N Pakkaranang, MU Rahmamn. Analysis of Food Chain Mathematical Model Under Fractal Fractional Caputo Derivative. *Mathematical Biosciences and Engineering*, 20(2):2094–2109, 2023.
[18] SM Ali Shah, H Tahir, A Khan, WA Khan, A Arshad. Stochastic Model on the Transmission of Worms in Wireless Sensor Network. *Journal of Mathematical Techniques in Modeling*, 1(1), 2024.
[19] A Din and Y Li. Optimizing HIV/AIDS Dynamics: Stochastic Control Strategies with Education and Treatment. *The European Physical Journal Plus*, 139(9):812, 2024.
[20] R Shafqat AND A Alsaadi. Artificial Neural Networks for Stability Analysis and Simulation of Delayed Rabies Spread Models. *AIMS Mathematics*, 9(12):33495–33531, 2024.
[21] A Din. Bifurcation Analysis of a Delayed Stochastic HBV Epidemic Model: Cell-to-Cell Transmission. *Chaos, Solitons Fractals*, 181:114714, 2024.
[22] A Turab, R Shafqat, S Muhammad, M Shuaib, MF Khan, M Kamal. Predictive Modeling of Hepatitis B Viral Dynamics: A Caputo Derivative-Based Approach Using Artificial Neural Networks. *Scientific Reports*, 14(1):21853, 2024.
[23] IS Onah, OC Collins, PG Uchechukwu Madueme, GC Ezike Mbah. Dynamical System Analysis and Optimal Control Measures of Lassa Fever Disease Model. *International Journal of Mathematics and Mathematical Sciences*, 2020(1):7923125, 2020.
[24] MA Ibrahim and A Dénes. A Mathematical Model for Lassa Fever Transmission Dynamics in a Seasonal Environment with a View to the 2017–20 Epidemic in Nigeria. *Nonlinear Analysis: Real World Applications*, 60:103310, 2021.
[25] OJ Peter, AI Abioye, FA Oguntolu, TA Owolabi, MO Ajisope, AG Zakari, TG Shaba. Modelling and Optimal Control Analysis of Lassa Fever Disease. *Informatics in Medicine Unlocked*, 20:100419, 2020.
[26] OB Salu, OS Amoo, JO Shaibu, C Abejegah, O Ayodeji, AZ Musa, I Idigbe, OC Ezechi, RA Audu, BL Salako, SA Omilabu. Monitoring of Lassa Virus Infection in Suspected and Confirmed Cases in Ondo State, Nigeria. *The Pan African Medical Journal*, 36(253), 2020.
[27] X Liao, LQ Wang, P Yu. *Stability of Dynamical Systems.* Elsevier, New York, 2007.
[28] JL Salle. *Stability by Liapunov's Direct Method with Applications.* Academic Press, 1961.
[29] PVD Driessche and J Watmough. Reproduction Numbers and Sub-Threshold Endemic Equilibria for Compartmental Models of Disease Transmission. *Mathematical biosciences*, 180(1-2):29–48, 2002.
[30] OC Collins and KS Govinder. Stability Analysis and Optimal Vaccination of a Waterborne Disease Model with Multiple Water Sources. *Natural Resource Modeling*, 29(3):426–447, 2016.

[31] Y Ramzan, AA Awan, M Ozair, T Hussain and R Mahat. Innovative Strategies for Lassa Fever Epidemic Control: A Groundbreaking Study. *AIMS Mathematics*, 8(12):30790–30812, 2023.

[32] C Castillo-Chavez, S Blower, P van den Driessche, D Kirschner, AA Yakubu. *Mathematical Approaches for Emerging and Reemerging Infectious Diseases: Models, Methods, and Theory*. Springer Science Business Media, New York, 2002.

[33] NCDC. An update of Lassa fever outbreak in Nigeria. https://ncdc.gov.ng/diseases/sitreps/?cat=5name=An accessed in April 2025.

[34] World Bank Group. Average life expectancy of Nigeria in 2018. https://data.worldbank.org/indicator/SP.DYN.LE00.IN?end=2018locations=NGstart=2018view=bar. accessed in April 2025.

[35] Charting The Globe. Total population of Nigeria in 2018. https://chartingtheglobe.com/demographics/population?indicator=populationregions=162visual=bar. accessed in April 2025.

[36] Charting The Globe. The female population in Nigeria in 2018. https://chartingtheglobe.com/region/nigeria/demographics/population?indicator=female-population. accessed in April 2025.

[37] Charting The Globe. The male population in Nigeria in 2018. https://chartingtheglobe.com/region/nigeria/demographics/population?indicator=male-population. accessed in april 2025.

[38] MM Ojo, B Gbadamosi, O Adebimpe, RO Ogundokun. Sensitivity Analysis of Dengue Model With Saturated Incidence Rate. *Biomath Communications Supplement*, 5:e4413, 2018.

[39] M Ojo and F Akinpelu. Sensitivity Analysis of Ebola Virus Model. *Asian Research Journal of Mathematics*, 2(3):1–10, 2017.

[40] LS Pontryagin. *Mathematical Theory of Optimal Processes*. Routledge, London, 2018.

[41] WH Fleming and RW Rishel. *Deterministic and Stochastic Optimal Control*. Springer Science Business Media, New York, 2012.

[42] H Hamam, Y Ramzan, S Niazai, KA Gepreel, AU Awan, M Ozair and T Hussain. Deciphering the enigma of lassa virus transmission dynamics and strategies for effective epidemic control through awareness campaigns and rodenticides. *Scientific Reports*, 14(1):18079, 2024.